Magnetic properties of anisotropic superconductors

Robert Joynt
Theoretische Physik, ETH-Hönggerberg, CH-8093 Zürich, Switzerland,
and Department of Physics, 1150 University Ave., University of Wisconsin, Madison, Wisconsin 53706

T. M. Rice
Theoretische Physik, ETH-Hönggerberg, CH-8093 Zürich, Switzerland
(Received 26 October 1987)

We calculate the frequency- and wave-vector-dependent particle-hole spin susceptibilities $\chi(\mathbf{q},\omega)$ of anisotropic superconductors, such as heavy-fermion and, possibly, high-T_c systems. This information is used to analyze the outcome of proposed neutron scattering experiments on these systems. It is found that the dependence of the cross sections on $\mathbf{q}$ can give detailed information about the anisotropic modification of the excitation spectrum. In addition, the polarization dependence of the cross section reflects directly the vector structure of the gap function, so that ultimately complete identification of a superconducting phase is possible. We discuss the implications of our results for the question of the relative thermodynamic stability of the various phases in the presence of external magnetic fields. A table of static susceptibilities for some possible phases of a cubic system with spin-orbit coupling is given. The large energy scales in high-T_c systems make them ideal for these experiments.

I. INTRODUCTION

The discovery of superconductivity in the heavy-electron metals[1-3] has led to intensive efforts to establish the precise nature of the superconducting state. In particular, a series of specific-heat and transport measurements have shown anomalous temperature dependences for these quantities. These have been interpreted as evidence that the magnitude of the gap vanishes somewhere on the Fermi surface.

However, there is no unanimity on the detailed interpretation of these experiments.[4-6] The possibilities advanced in the literature range from conventional s-state superconductivity with strong depairing effects to zeros of the magnitude of the gap at specific points on the Fermi surface (axial case) and zeros at lines on the Fermi surface (polar case). Progress in the clarification of these issues is difficult for two reasons. The order parameter does not couple directly to external probes and the thermodynamic and transport properties give, at best, evidence of the energy dependence of the excitation spectrum rather than a direct measurement of the order parameter. Secondly, the properties of the normal state of these complex materials are not known in detail. This compounds the difficulties in deriving a consistent interpretation of the experiments on the superconducting state.

Recently superconductors have been discovered which have high critical temperatures and other remarkable properties.[7,8] There are strong theoretical reasons for believing that superconductivity in the high-T_c copper oxide systems is anisotropic, with d-wave symmetry.[9-11] Experimental evidence for or against this viewpoint is so far inconclusive and we suggest a new approach to this problem.

Very important for the solution of these difficulties is a knowledge of $\chi^S(\mathbf{q},\omega)$, the wave-vector- and frequency-dependent susceptibility in the superconducting state. The superconducting correlations change χ very strongly at frequencies corresponding to the gap energy Δ. These correlations can be observed in neutron scattering experiments, which can have *energy* resolutions approaching 0.1 meV. Such resolution is adequate for the heavy-fermion systems ($\Delta \sim 0.1$ meV) and much more than adequate for high-T_c materials ($\Delta \sim 10$ meV). On the other hand, it will be seen below that the detection of the most interesting effects requires only relatively coarse (~ 1 Å^{-1}) resolution in the wave vector. We shall also show that neutron experiments have the potential, in principle, to determine the order parameter completely.

Experiments[12] on UPt_3 have so far been carried out at energy resolutions exceeding 1 meV. At frequencies corresponding to this energy the spin correlations are antiferromagnetic, with the two U moments in the unit cell aligned antiparallel. More interesting, for our purposes, is the nature of the extrapolation of these measurements to zero frequency ω. This extrapolation suggests that the frequency linewidth as a function of momentum transfer $\mathbf{q}$ does not vanish as $\mathbf{q}\rightarrow\mathbf{0}$, in contradiction to Fermi-liquid theory. Since there are many other indications that UPt_3 is a Fermi liquid,[13] this strongly suggests that the extrapolation is not valid. This is to be expected in any case, since 1 meV is comparable to the estimated Fermi energy of UPt_3. The periodic Anderson model of heavy Fermi liquids will give finite-frequency (interband) contributions, but the low-frequency (intraband) part must always satisfy Fermi-liquid theory. In particular, the limit of low frequencies and long wavelengths must have the usual renormalized particle-hole form. In this paper we deal only with this low-frequency part of the

spectrum; it is, in any case, the only part which is modified by superconductivity. This is analogous to the situation in ordinary electron-phonon superconductors,[14] where modification of the low-energy phonon spectrum in Nb_3Sn has been observed by neutron scattering. Section II is devoted to the discussion of $\mathrm{Im}\chi(\mathbf{q},\omega)$ when spin-orbit coupling is neglected. Section III treats this coupling.

The static uniform susceptibility is also of interest since it may influence stability in the presence of strong external fields, $H_{c1}<H<H_{c2}$. One will then have spatially inhomogeneous configurations of the order parameter. Since the London limit, penetration depth much larger than coherence length, is usual in the systems of interest, there will be large regions where field penetration and superconductivity coexist. There will then be a contribution to the energy of the form $-\frac{1}{2}\sum_{i,j} H_i\chi_{ij}H_j$. This term must be considered in addition to the usual ones which determine the structure of the inhomogeneous states. Its effect is treated in Sec. IV. A table of uniform susceptibilities for some important cubic phases is also presented there. Section V is given over to an evaluation of the assumptions made in our calculations, possible improvements of these, and finally some conclusions.

We concentrate throughout on the examples of UBe_{13}, a cubic system, and ^{3}He. These have the advantage that the underlying system is relatively isotropic, so that spontaneous breaking of rotational symmetry is easier to disentangle from effects due only to anisotropic crystal structure. In particular, ^{3}He has full rotational symmetry and is therefore, very convenient for theoretical analysis. Neutron scattering in the superfluid phase is unfortunately very difficult experimentally. Finally, we assume that all samples consist only of a single domain, if they are anisotropic triplet superconducting systems. This can probably be achieved experimentally by cooling the sample in an external magnetic field.

II. NEUTRON SCATTERING CROSS SECTIONS

We wish to calculate the spin susceptibility in a triplet superconducting state, where the gap parameter is allowed to be a function of angle $\hat{\mathbf{k}}$ on the Fermi surface and is a 2×2 matrix. Our interest will be in the particle-hole susceptibility, neglecting impurity effects and spin-orbit coupling. The latter is discussed in the following section. The usual Gor'kov decoupling is employed, which leads to the following expression for χ in terms of Δ:

$$-\frac{1}{\mu_B^2}\chi_{ij}(\mathbf{q},i\omega)=\sum_{\mathbf{k}}\frac{C_{ij}(\mathbf{k},\mathbf{q})}{i\omega-E_+-E_-},\quad \omega\geq 0\ . \tag{1}$$

Here μ_B is the Bohr magneton, and

$$E_\pm^2(\mathbf{k},\mathbf{q})\equiv(\varepsilon_{\mathbf{k}\pm\mathbf{q}/2}-\mu)^2+\tfrac{1}{2}\mathrm{Tr}[\Delta^\dagger(\mathbf{k}\pm\mathbf{q}/2)\Delta(\mathbf{k}\pm\mathbf{q}/2)]\ ,$$

where ε is the band energy and μ is the Fermi energy, $C_{ij}(\mathbf{k},\mathbf{q})$, the coherence factor, is given by

$$C_{ij}(\mathbf{k},\mathbf{q})=\frac{\frac{1}{2}\delta_{ij}[(E_++\xi_+)(E_--\xi_-)+\mathrm{Re}(\mathbf{d}_+^*\cdot\mathbf{d}_-)]-\mathrm{Re}(d_{i+}^*d_{j-})}{E_+E_-} \tag{2}$$

with $\xi_\pm=\varepsilon_\pm-\mu$, for the case of triplet superconductivity. We have introduced $\mathbf{d}(\hat{\mathbf{k}})$, defined by the equation

$$\Delta(\hat{\mathbf{k}})=i\boldsymbol{\sigma}\cdot\mathbf{d}(\hat{\mathbf{k}})\sigma_y\ .$$

$\mathbf{d}$ is a convenient quantity to work with since it transforms as a vector under the operations of the rotation group, whether this group is continuous as in the case of ^{3}He, or discrete, as in the case of a crystal point group. The σ's are the usual Pauli matrices. For a derivation of (1) and (2) see, e.g., Ref. 15. These equations are valid, strictly speaking, only for the so-called unitary case: $\mathbf{d}\times\mathbf{d}^*=0$. This is the case which will be most important, and even for the nonunitary states it can be shown that there are no corrections to first order in $\mathbf{d}\times\mathbf{d}^*$ to (1).[16]

A magnetic property accessible to neutron scattering is the function $\mathrm{Im}\chi_\pm(\mathbf{q},\omega+i\delta)$, which is proportional to the spin-flip scattering cross section, when the incoming beam is polarized in the z direction. This quantity is given by Eq. (1) with C_{ij} replaced by

$$C_\pm(\mathbf{k},\mathbf{q})=[(E_++\xi_+)(E_--\xi_-)+\mathrm{Re}(d_{z+}d_{z-}^*)]/4E_+E_- \tag{3}$$

and $(i\omega-E_+-E_-)^{-1}$ replaced by $-\pi\delta(\omega-E_+-E_-)$.

Also easily calculable from (1) is $\mathrm{Im}\,\mathrm{Tr}_i\chi_{ii}(\mathbf{q},\omega+i\delta)$, which in an isotropic system would be proportional to the neutron scattering cross section for unpolarized incident beam and outgoing polarization not observed, with the nonmagnetic scattering subtracted and ignoring kinematical factors. This quantity is also of interest in connection with the spin-fluctuation energy. To obtain it, we must replace C_{ij} in (1) by C_T, where C_T is determined from

$$C_T=[\tfrac{3}{2}(E_++\xi_+)(E_--\xi_-)+\tfrac{1}{2}\mathrm{Re}(\mathbf{d}_+\cdot\mathbf{d}_-^*)]/E_+E_-\ . \tag{4}$$

For general directions of the momentum transfer $\mathbf{q}$, the sum in Eq. (1) is difficult to carry out by hand and numerical computation is required. This is done for a range of frequencies less than a cutoff of about five times the root-mean-square gap frequency by sampling the region of momentum space near the Fermi surface which includes all possible transitions having frequency less than the cutoff. The points are classified according to their frequency with a bin width of about 0.2 times the root mean square gap. The coherence factor is then evaluated for each. In this way the entire function can be constructed

for frequencies below the cutoff. Above the cutoff, the susceptibility goes over quickly to its normal state value. Δ_m, the maximum value of the gap, is chosen as $0.0525\varepsilon_F$, where ε_F is the Fermi energy. This ratio corresponds very roughly to T_c/ε_F in UBe_{13}. For the band structure we use a linear dispersion $\varepsilon = v_F |\mathbf{k}|$, which has a spherical Fermi surface. This would correspond reasonably well with the Γ-centered piece of the Fermi surface in UPt_3, for example. Of course, real comparison of theory and experiment would require experimental identification of the different pieces of the surface and would be more complicated than the simple pilot calculations presented here. Because of this neglect of the real band structure, and because the main interest is in how the superconductivity modifies the susceptibility, we prefer to plot in most instances $\mathrm{Im}\chi^S(\mathbf{q},\omega)/\mathrm{Im}\chi^N(\mathbf{q},\omega)$, the ratio of the superconducting and normal susceptibilities. $\mathrm{Im}\chi^N(\mathbf{q},\omega)$ is computed from the above dispersion law. In the low-energy regime, however, it does not differ materially from the usual Lindhard form. We caution the reader that in this model the intensity at low energy falls off rather quickly at high q in the normal phase. So if this model is close to the correct one, the effects that we calculate will be more difficult to observe as $\mathbf{q}$ increases. In addition antiferromagnetic correlations arising from interactions may be present in the intraband part of χ.

At $q=0$, the integrals defining χ^S may be performed analytically. For orientation, we plot $\mathrm{Im}\,\mathrm{Tr}\chi(0,\omega)$ in Fig. 1 for the polar $[\mathbf{d}\sim\hat{\mathbf{x}}(k_x+ik_y)]$ phases. This diagram is simply meant to show the nonanalytic behavior at $2\Delta_m$, where $2\Delta_m$ is twice the maximum value of the gap. At finite q the logarithmic divergence of the susceptibility of the ABM phase is cut off. The behavior at small frequencies, linear for the polar phase and quadratic for the ABM, is just due to the line of zeros at the equator and the point zeros at the poles in the two respective cases. Both the position of the maximum and the low-frequency behavior will in general change at finite q in both cases.

We will investigate only these two phases below as examples of triplet superconductors. It should be noted, however, that neither phase is possible in a cubic crystal with strong spin-orbit coupling.[17–20] They are both stable solutions for an isotropic system like ^{3}He, but T_c, and hence, the gap is so small in ^{3}He that neutron scattering investigations of its superfluid correlations are at present, out of the question. Since our aim here is mainly to illustrate how physical information may be extracted from neutron results, we feel justified in using the simplest, rather than the most likely, candidates for heavy-fermion superconducting phases. The number of the latter is in any case rather large (see Table I). An example of a d-wave phase, the three-dimensional analogue of proposed phases for high-T_c systems, is also treated.

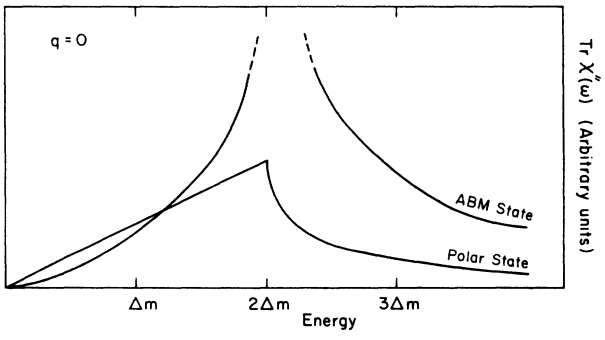

FIG. 1. The imaginary part of the averaged susceptibility $\mathrm{Tr}\chi''(0,\omega)$ at zero momentum transfer. These functions reflect the density of states in the two phases shown. In particular, the ABM phase has a singularity at twice the value of the gap at the equator of the Fermi surface.

In Fig. 2, the numerically calculated results in the polar phase for $\mathrm{Im}\,\mathrm{Tr}\chi(\mathbf{q},\omega)$ (dashed curves) and $\mathrm{Im}\chi_{\pm}(\mathbf{q},\omega)$ (solid curves) are shown for $\hat{\mathbf{q}}$ in the [110] direction. Several features of the curves are noteworthy. The first is that the position of the maximum is q dependent. To understand the reason for this, think first of the normal state. As q increases, the low-energy transitions are confined increasingly to the equatorial plane, since $\mathbf{q}$ must span the Fermi surface. However, as $\mathbf{q}$ squeezes down into this plane, the gap is decreasing until finally it goes to zero, and the maximum moves to small frequency. An attempt is made to illustrate this reasoning in the inset to Fig. 2. The circle is a cross section of the Fermi surface. The oval around it represents the magnitude of the gap as a function of the position on this surface. The equator, also shown, is the line on which the gap vanishes. The lowest-energy transitions for the different q's are shown as arrows.

Secondly, note the difference between spin-flip scattering in the z direction and the scattering averaged over spin directions. The former has an enhanced coherence factor, as may be seen from formulas (3) and (4) given above. (Note that $\mathbf{d}_+ = \mathbf{d}_-$ for this case since $\mathbf{q}$ is perpendicular to $\hat{\mathbf{z}}$.) While the motion of the maximum of χ reflects the $\hat{\mathbf{k}}$ dependence of $\mathbf{d}$ ($\mathbf{d}$ a function only of k_z),

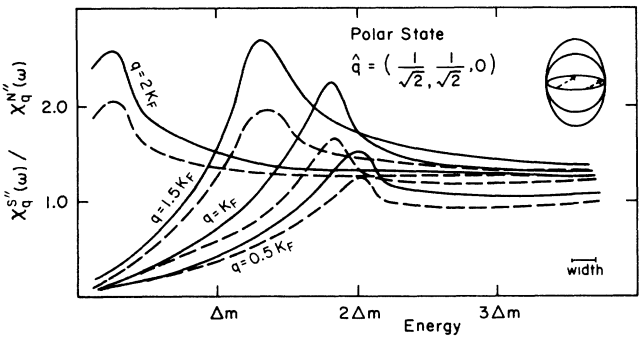

FIG. 2. The imaginary part of the polar phase z-polarized spin-flip susceptibility $\chi''_{\pm}(\mathbf{q},\omega)$ (solid curves), and the averaged spin-flip susceptibility $\mathrm{Tr}\chi''(\mathbf{q},\omega)$ (dashed curves). These are shown as functions of ω for selected values of q, when $\mathbf{q}$ is in the [110] direction. $\Delta_m = 0.0525\varepsilon_F$, where ε_F is the Fermi energy. $\hbar = 1$. The inset shows some possible transitions having low energy for two values of q. The circle represents a cross section of the Fermi surface and the oval is a schematic picture of the gap magnitude on this surface.

TABLE I. This table lists the diagonal components χ_{xx}, χ_{yy}, and χ_{zz} and the maximum eigenvalue χ_m of the static uniform spin susceptibility tension for some triplet superconducting phases. For each of these, the off-diagonal components are all equal. In particular all off-diagonal elements are zero for the polar and ABM phases and for phases 1–9. For phases 10, 11, 12, and 13, the off-diagonal elements are $\frac{1}{6}$, $(2\pi/9\sqrt{3})-\frac{1}{2}=-0.097$, $\frac{2}{3}-\pi/4=-0.119$, and $\ln(\sqrt{3/2}+\sqrt{5/2})/3\sqrt{15}=0.89$, respectively. Also $c_1=1/\sqrt{2}+i/\sqrt{6}$, $c_2=-1/\sqrt{2}+i/\sqrt{6}$, and $c_3=-2i/\sqrt{3}$. χ_P is the Pauli susceptibility of the normal phase.

Name and/or number	$\mathbf{d}(\hat{\mathbf{k}})$	χ_{xx}	χ_{yy}	χ_{zz}	χ_m
Polar	$\hat{\mathbf{z}}k_z$	1	1	0	1
ABM	$\hat{\mathbf{x}}(k_x+ik_y)$	0	1	1	1
1,BW	$\hat{\mathbf{x}}k_x+\hat{\mathbf{y}}k_y+\hat{\mathbf{z}}k_z$	$\frac{2}{3}$	$\frac{2}{3}$	$\frac{2}{3}$	$\frac{2}{3}$
3	$2\hat{\mathbf{z}}k_z-\hat{\mathbf{x}}k_x-\hat{\mathbf{y}}k_y$	$\frac{7}{6}-\frac{2\pi}{9(3)^{1/2}}=0.764$	0.764	$\frac{4\pi}{9(3)^{1/2}}-\frac{1}{3}=0.473$	0.764
4	$\hat{\mathbf{x}}k_x-\hat{\mathbf{y}}k_y$	$\frac{1}{2}$	$\frac{1}{2}$	1	1
5	$e^{-2\pi i/3}\hat{\mathbf{x}}k_x+e^{2\pi i/3}\hat{\mathbf{y}}k_y+\hat{\mathbf{z}}k_z$	$\frac{2}{3}$	$\frac{2}{3}$	$\frac{2}{3}$	$\frac{2}{3}$
6	$\hat{\mathbf{x}}k_y-\hat{\mathbf{y}}k_x$	$\frac{1}{2}$	$\frac{1}{2}$	1	1
7	$\hat{\mathbf{x}}k_y+\hat{\mathbf{y}}k_x$	$\frac{1}{2}$	$\frac{1}{2}$	1	1
8	$\hat{\mathbf{x}}(k_y-ik_z)+(\hat{\mathbf{y}}-i\hat{\mathbf{z}})k_x$	$2-\frac{\pi}{2}=0.427$	$\frac{\pi}{4}=0.786$	0.786	0.786
9	$\hat{\mathbf{x}}(k_y+ik_z)-(\hat{\mathbf{y}}+i\hat{\mathbf{z}})k_x$	0.427	0.786	0.786	0.786
10	$\hat{\mathbf{x}}(k_y-k_z)+\hat{\mathbf{y}}(k_z-k_x)+\hat{\mathbf{z}}(k_x-k_y)$	$\frac{2}{3}$	$\frac{2}{3}$	$\frac{2}{3}$	1
11	$\hat{\mathbf{x}}(k_y+k_z)+\hat{\mathbf{y}}(k_z+k_x)+\hat{\mathbf{z}}(k_x+k_y)$	$\frac{2}{3}$	$\frac{2}{3}$	$\frac{2}{3}$	0.764
12	$\hat{\mathbf{x}}(c_2k_z-c_3k_y)+\hat{\mathbf{y}}(c_3k_x-c_1k_z)+\hat{\mathbf{z}}(c_1k_y-c_2k_x)$	$\frac{2}{3}$	$\frac{2}{3}$	$\frac{2}{3}$	0.786
13	$\hat{\mathbf{x}}(c_2k_z+c_3k_y)+\hat{\mathbf{y}}(c_3k_x+c_1k_z)+\hat{\mathbf{z}}(c_1k_y+c_2k_x)$	$\frac{2}{3}$	$\frac{2}{3}$	$\frac{2}{3}$	0.855

the polarization dependence reflects the vector structure of $\mathbf{d}$ ($\mathbf{d}$ in the z direction). This is a general feature of our results and demonstrates that neutron scattering is a unique tool for probing the *vector* nature of the order parameter. No other experiment seems capable of offering this sort of detailed information. Also important is the fact that the interesting structure is apparent on the very coarse scale of momentum $q\sim K_F$, or wavelengths of the order of angstroms. Good energy resolution is required for heavy-fermion systems, however, of the order of $2\Delta_m$, which in UBe_{13} is probably about 0.5 meV.

Figure 3 shows the same state but with $\mathbf{q}$ now in the z direction. The contrast with the [110] direction is very marked. Here the maximum is completely washed out in the $\chi_\pm$ curves. In both polarized and averaged curves we see a gap developing as we increase q. This may be understood by an argument like that given for the [110] direction. As q increases, low energy transitions are confined to the tube connecting the north and south poles. However, this sort of process faces the maximum energy to break a pair, $2\Delta_m$, as $q\rightarrow 2K_F$. Such a transition is shown in the inset to Fig. 3, along with one of smaller q. Thus, the gap which was absent at $q=0$, (Fig. 1), develops as q increases only if it does so in a direction in which the magnitude of the $\mathbf{d}$ is increasing.

Another striking feature of Fig. 3 is the difference between z polarized and averaged cross sections. To understand this, consider Eq. (3) for $C_\pm$ and set $\mathbf{q}=(0,0,2K_F)$. The transitions of lowest energy have $\xi_+\approx\xi_-$ and $d_+\approx d_-$ because these transitions connect $(0,0,-K_F)$ and $(0,0,K_F)$. We then have $(E_+-\xi_-)\approx d_+^2$ and $C_\pm\approx 0$, because the two terms in the numerator cancel. In general a spin-flip transition between points where $k_z(\text{final})=-k_z(\text{initial})$ is forbidden. Such a strong polarization suppression is therefore a sign that (a) the polarization is parallel, or nearly parallel, to the direction of $\mathbf{d}$ and (b) that there is a change of sign of the parallel component of $\mathbf{d}$ involved in the transition.

In this polar phase, for a general direction, we expect to see a crossover from the behavior of Fig. 2 to that of Fig. 3 as q_z increases. The gap is $2\Delta_m(q_z/2K_F)$, but the edge will not be so sharp if $\mathbf{q}$ also has components in the x-y plane. The crossover to suppressed polarized cross section occurs first at larger k_z if k_x, say, is appreciably

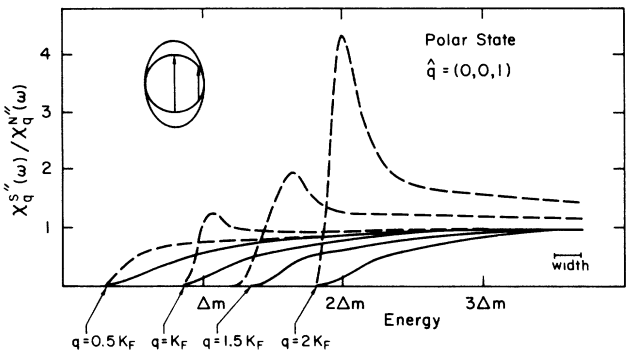

FIG. 3. Polarized (solid curves) and averaged (dashed curves) imaginary susceptibilities χ'' for the polar phase when $\mathbf{q}$ is in the [001] direction. The inset shows possible transitions for two values of q. No transitions of finite q can connect points where the $\mathbf{d}$ vanishes.

large, since only then will most low-energy transitions involve scattering across the equatorial plane.

We now turn to the ABM phase. The cross sections for $\hat{\mathbf{q}}$ in the [110] direction are shown in Fig. 4. Again we see the development of a gap as q increases, just as in Fig. 3, and for similar reasons. Two transitions belonging to $q=2K_F$ and $q=K_F$ are shown in the inset. The gap in the spectrum is again a linear function of q, for the same reason as before. The position of the maximum, however, sticks at $2\Delta_m$. This is a remnant of the strong $q=0$ singularity, and is due to the fact that the equatorial plane always contains some transitions. In this diagram, we see clearly a crossover from enhancement to suppression of the averaged cross section. Since this contains the spin-flip cross section for the x direction (i.e., parallel to $\mathbf{d}$) it will be suppressed when k_x and k_y change sign in the transition. For small q this is not the case for most transitions since they occur near the $k_x=-k_y$ plane. For $q=2K_F$, on the other hand, the low-energy transitions span the points $k_F(-1/\sqrt{2},-1/\sqrt{2},0)$ and $K_F(1/\sqrt{2},1/\sqrt{2},0)$, and x spin flips are suppressed by the coherence factor. Hence, the crossover.

Figure 5, with $\hat{\mathbf{q}}$ in the [001] direction, also shows a q dependent gap. This now *decreases* as q increases since the possible transitions move from the neighborhood of the equator where the gap is maximum, to the poles where it is minimum. This is illustrated in the inset. The peak position is also a function of q since all low-energy transitions connect points with equal values of the order parameter. The peak position is given by $2\Delta_m[1-q/2K_F)^2]^{1/2}$. In this case there is no change in sign of d in the transition and the x spin flip is always enhanced, and the averaged cross section is always larger than the z polarized one.

We can conclude that the ABM and polar phases differ qualitatively from the experimental point of view. The ABM state has a gap for pair breaking at all finite q. For the polar phase this is true only if $\mathbf{q}$ is parallel to $\mathbf{d}$.

Our final example is a singlet anisotropic state. If the gap falls into an even representation of the crystal point group such states are possible, and some of them are

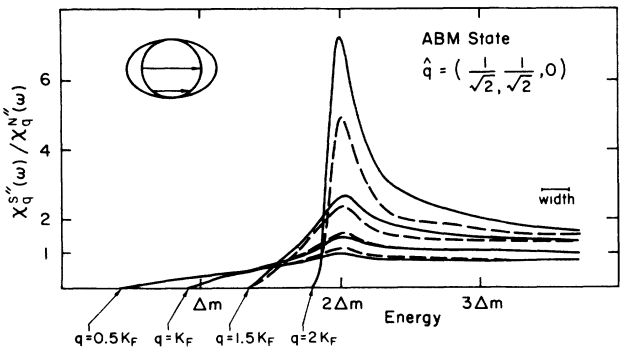

FIG. 4. Polarized (solid curves) and averaged (dashed curves) imaginary susceptibilities χ'' for the ABM phase, for $\mathbf{q}$ in the [110] direction. The inset shows lowest-energy transitions for two values of q. The energy involved in these is an increasing function of q. Again $\Delta_m=0.0525\varepsilon_F$.

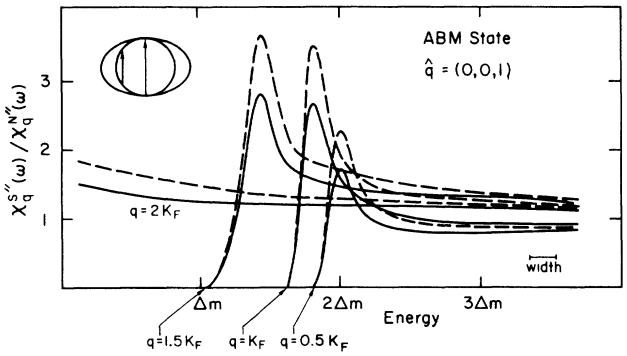

FIG. 5. Polarized (solid curves) and averaged (dashed curves) imaginary susceptibilities χ'' for the ABM phase, for $\mathbf{q}$ in the [001] direction. Some possible transitions are illustrated in the inset. In this case the energy involved decreases as q increases.

given by Volovik and Gor'kov.[18] Such states have been proposed for heavy-fermion systems by several authors,[21] since they are stabilized by anitiferromagnetic correlations. For all singlet states the order parameter is a single function of $\hat{\mathbf{k}}$, the direction on the Fermi surface. BCS theory need only be modified to take into account the orbital anisotropy of the Cooper pair wave function. The pairs are rotationally invariant in spin space. One can immediately conclude that there is no polarization dependence of the cross section. Also at $T=0$, the uniform, static susceptibility vanishes under the assumptions made here. It then follows from the Kramers-Kronig relation: $\mathrm{Re}\chi(0,0)=(2/\pi)\int_0^\infty[\mathrm{Im}\chi(0,\omega)/\omega]d\omega$ and $\mathrm{Im}\chi(0,\omega)\geq 0$ for $\omega\geq 0$ that the absorptive part of the susceptibility vanishes for all frequencies at $q=0$. It is clear that there are very strong qualitative differences between singlet and triplet phases.

Density-of-states effects are still detectable in singlet phases. We give the results to be expected from an analysis of different $\hat{\mathbf{q}}$ directions in the phase characterized by $\Delta\sim k_xk_y$. Figure 6 shows χ for q in the [110]

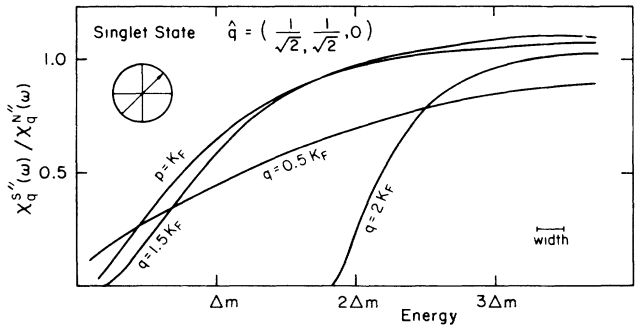

FIG. 6. Imaginary part of the susceptibility χ'' for a singlet state with gap function proportional to k_xk_y, where k_x and k_y are components of the momentum on the Fermi surface. Here $\mathbf{q}$ is in the [110] direction. A cross section of the Fermi surface is shown in the inset, with lines of zeros of the order parameter indicated. A $q=2K_F$ transition is illustrated. It connects points where the gap is maximized. $\Delta_m=0.0525\varepsilon_F$.

direction. For small q we see the coherence factor suppression, which persists out to rather high frequencies. At $q=K_F$, this is no longer important. At $q=1.5K_F$, a gap has begun to develop, owing to the fact that the largest wave vector which can connect two points where the order parameter is zero is actually $q=\sqrt{2}K_F$, which joins $(-K_F,0,0)$ and $(0,K_F,0)$. At $q=2K_F$ the gap is fully developed, the lowest-energy transition being shown in the inset, which is a view along the z axis with lines of zeros being indicated.

Figure 7 shows the results for q in the [001] direction. Again the increase of $\mathrm{Im}\chi$ with increasing q is clear. Here, however, there is no gap for any value of q, since transitions lying entirely in the $k_x=0$ or $k_y=0$ planes are always possible. For the high-temperature superconductors, a d wave state has been proposed by some authors.[9–11] The gap is given by $\Delta=\Delta_0(\cos k_x a-\cos k_y a)$, where a is the lattice constant in a two-dimensional square lattice. For wave vectors lying in this plane, we will see a gap open up in $\chi(\mathbf{q})$ only if q lies along the crystal axes. If $\mathbf{q}$ is along a diagonal, the gap vanishes.

We conclude that neutron scattering is capable of probing all of the aspects of the very rich symmetry-breaking characteristic of triplet superconductors. In addition it is capable of distinguishing the qualitative differences between triplet and singlet phases.

III. SPIN-ORBIT COUPLING AND SMALL-ANGLE SCATTERING

The effects of spin-orbit coupling are far reaching. The eigenstates are no longer eigenfunctions of the spin components and coupling of the neutron to the orbital motion of the electron must be taken into account. The summand in Eq. (1) will include a factor

$$\frac{1}{\mu_B^2}\langle \mathbf{k}-\mathbf{q}/2\ \alpha\,|\,L_i+2S_i\,|\,\mathbf{k}+\mathbf{q}/2\ \beta\rangle \langle \mathbf{k}+\mathbf{q}/2\ \beta\,|\,L_j+2S_j\,|\,\mathbf{k}-\mathbf{q}/2\ \alpha\rangle\ . \quad (5)$$

Here α and β are pseudospin labels obtained by turning on the spin-orbit coupling adiabatically and L_i, S_i are the appropriate components of the orbital and spin angular momentum. Hence, the average in Eq. (1) is weighted by this factor as well as the coherence factor. Unfortunately not too much is known about these matrix elements. There have been calculations of the diagonal terms in a simplified model,[22] which tell us that the effective moments are strong functions of direction on the Fermi surface. This is likely to be true also in real materials.

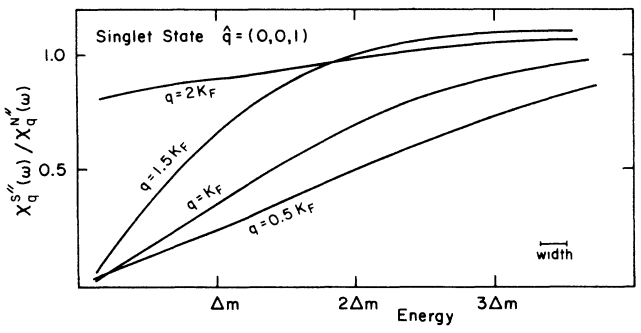

FIG. 7. Imaginary part of the susceptibility χ'' for the singlet state with $\mathbf{q}$ in the [001] direction.

This effect will show up in the normal state as directional dependence of the scattering cross section even for an isotropic Fermi surface. In the superconducting state it is possible that there are correlations between regions of high effective moment and large gap on the Fermi surface. This would enhance the movement of weight to higher frequencies in the superconducting state, making anisotropies easier to observe. Unfortunately, it also makes them more difficult to interpret. In the absence of a complete strong-coupling theory and band calculations of the relevant matrix elements it would not be possible to deduce much detailed information about the gap function from such an enhancement.

One case in which the spin-orbit effect can be partially eliminated is for scattering at small $\mathbf{q}$, $|\mathbf{q}|\ll K_F$. This kind of experiment has the additional advantage that phonon scattering cross sections are very small so that magnetic scattering is more easily separated from nuclear scattering. Also the coherence factors of Eqs. (3) and (4) simplify: for the polar phase, $C_\pm=C_T=\Delta^2/2E^2$ and for the ABM phase, $C_\pm=C_T/2=\Delta^2/4E^2$. There are no dramatic interference effects possible, as the entire Fermi surface contributes to the lower-energy spectrum. Also, and just as importantly, the matrix elements (5) are averaged over.

The chief results as $\mathbf{q}$ is increased from zero are tabulated in Table II. The changes in threshold energies are not modified from the results of the previous section. The power-law dependences are not affected at finite q, e.g., the cross section still rises linearly in ω from the threshold value for the polar phase and as ω^2 for the ABM phase. If $q\ll K_F$ the threshold frequencies are of course small. The change in position of the $q=0$ singularity for each case may also be verified by comparing the results in the table to the $q=0.5K_F$ curves in Figs. 2–5. In general, if $\mathbf{q}$ is parallel to the gap surface where the gap is at a maximum, as in the insets to Figs. 2 and 5, then the singularity remains at $\omega=2\Delta_m$. If $\mathbf{q}$ is perpendicular to the surface, then the singularity moves up in frequency, is quickly weakened, and in fact is off scale in Figs. 3 and 4. Note that in this connection the peaks in Figs. 3 and 4 represent the development at large q of a threshold frequency, not to be confused with the long-wavelength peak of Fig. 1. The anisotropy of the movement of the singularity is probably the feature most experimentally accessible at low q, since it occurs at a finite frequency and can therefore, be distinguished from elastic events.

All of the *qualitative* features mentioned in this section are independent of the existence of spin-orbit coupling, since they are essentially density-of-states effects. The only possible exception would be extraordinary behavior of the matrix elements (5) such as the vanishing of the effective moment where the gap is maximum, etc. This is rather unlikely.

TABLE II. Behavior of frequency dependent cross sections at small q, $q \ll K_F$. The two most prominent features in the cross sections, the threshold frequencies and singularity frequencies, may change position as q is increased. These changes are anisotropic.

	Polar		ABM	
	$\sqrt{2}\hat{\mathbf{q}}=(1,1,0)$	$\hat{\mathbf{q}}=(0,0,1)$	$\sqrt{2}\hat{\mathbf{q}}=(1,1,0)$	$\hat{\mathbf{q}}=(0,0,1)$
Singularity frequency	$2\Delta_m$	$(4\Delta_m^2+v_F^2q^2)^{1/2}$	$(4\Delta_m^2+v_F^2q^2)^{1/2}$	$2\Delta_m$
Threshold frequency	0	$\Delta_m q/K_F$	$\Delta_m q/K_F$	0

Small-angle scattering in the d-wave state is of little interest. The $q=0$ cross section vanishes for all frequencies, as already noted. Spin-orbit coupling cannot change this. As long as the Cooper-pair orbital wave function has even parity, the coupling to a static magnetic field must vanish to first order.

IV. STATIC SUSCEPTIBILITY

The results for the tensor $\chi_{ij}=\mathrm{Re}\chi_{ij}(0,0)$ are given in Table I for the polar, ABM and Balian-Werthamer (BW) phases along with some of the possible triplet phases of a cubic crystal with strong spin-orbit coupling, as given in Refs. 12–15. These are obtained from the appropriate limit of Eq. (1), which neglects spin-orbit matrix elements. The integrals may all be performed analytically since the density-of-states part of the integrand depends essentially on $|\mathbf{d}|^2$, which is a quadratic function of the components of $\mathbf{k}$, where $\mathbf{k}$ is the integration variable. This can always be diagonalized by an orthogonal transformation. Note that all phases satisfy the identity $\mathrm{Tr}\chi=\frac{2}{3}\chi_P$, where χ_P is the Pauli susceptibility. This corresponds to the fact that $\frac{2}{3}$ of the components of the triplet have a net projection on an axis, once orientations of the axis have been averaged over. χ always vanishes for d-wave superconductivity.

In ^{3}He in zero field, the ABM phase is stable only at high pressures and temperatures, relative to the BW phase. At high fields, the transition temperature between the two decreases, indicating that the ABM phase is becoming more favored energetically. In ^{3}He the phases have a continuous rotational degeneracy. In particular, they are free, if not near a boundary, to rotate the orientation of the order parameter into a direction such that the external magnetic energy $-\frac{1}{2}\sum_{ij}\chi_{ij}H_iH_j$ is minimized. Therefore, one finds an energy $-\frac{1}{2}\chi_m H^2$, where χ_m is the maximum eigenvalue of the susceptibility tensor. The orientation is along the principal axis belonging to this eigenvalue. The fact that $\chi_m(\mathrm{ABM})>\chi_m(\mathrm{BW})$ immediately explains the behavior in the field.

In the cubic case with spin-orbit coupling we have the twelve phases listed identified by the serial numbers assigned to them by Blount.[20] Physically, the situation in an external field is very different from ^{3}He since we are now dealing with a charged superfluid. For $H>H_{c1}$ and $T=0$, we have a mixed state where the vortices have small core radii ($\xi\sim 50$–100 Å) but large electromagnetic radii ($\lambda\sim 500$ Å). Thus, the usual Ginzberg-Landau equations describing this state must be supplemented by the external magnetic-field term. In addition, the fourth order and gradient terms for cubic symmetry and a vector order parameter are much more complicated than one usually has.[18] The problem is thus, quite difficult in general, combining the complexity of the Abrikosov vortex lattice with that of textures in ^{3}He. We do not attempt to solve it here, being content to point out that for $H\geq 2H_{c1}$, flux penetration is essentially complete, and only a small fraction passes through normal regions. In the crystalline case the order parameter is locked to the crystal axes, and stability is therefore determined by the full tensor expression and may depend on the direction of the field.

Finally, we observe that some of the states break time-reversal symmetry, namely 5, 8, 9, 12, and 13. These can, in principle, have an energy which is first order in H. The actual moment tends to cancel on averaging over the Fermi surface. These phases are good candidates for the low-temperature phase of $U_{1-x}Th_xBe_{13}$, $x>0.02$. Muon experiments indicate a small moment for this phase.[23]

V. CONCLUSION

Our basic aim in this paper was to calculate the intraband particle-hole susceptibility in the superconducting state of heavy-fermion systems. This means that we have neglected collective effects in this quantity entirely. We certainly expect that spin-wave modes, arising from the phase degree of freedom in the various components of the order parameter, will occur just as in ^{3}He. In ^{3}He, these modes have an energy v_Fq at small q. Spin-orbit coupling will create a gap at $q=0$ for these excitations in the cubic system, however, which will probably be of the same order as the superconducting gap, and will complicate the particle-hole spectrum we have given.

Spin-orbit coupling is known to have a strong effect on even the static susceptibility in BCS superconductors, as measured by the Knight shift in small samples.[24] This occurs when the spin-orbit scattering rate $1/\tau_{\mathrm{s.o.}}$ is so large that superconducting correlations cannot be established in such a short time: $\Delta\tau_{\mathrm{s.o.}}/h\ll 1$. In a system such as UBe_{13}, where the original eigenfunctions are presumably not spin eigenfunctions, collisions will erase spin memory, and $\tau_{\mathrm{s.o.}}$ is simply τ, the relaxation time. With a mean-free path of 1000 Å, we obtain an estimate of τ as 10^{-10} sec, and find $\Delta\tau/h\sim 1$. This highlights the importance of using very pure samples for any neutron work designed to see the preceding calculated effects. In addition, anisotropic superconductors are more prone to gaplessness than conventional ones.[25] Any such effect would also tend to wash out superconducting structure in the susceptibility. In the case of high-temperature superconductors, the neglect of spin-orbit coupling is well

justified, since atoms of lower atomic number are the only ones involved in the conduction bands.

Our results have been limited to the zero-temperature case. At finite temperatures two main effects will modify the results, aside from thermal smearing. One is simply that the size of the order parameter decreases. The structures which we identified as dependent on this quantity, such as gaps in certain directions for the scattering cross sections, will scale with the order parameter as it changes. The other is that scattering of thermally excited quasiparticles is now allowed in addition to the breaking of Cooper pairs. This effect will fill in gaps in the spectra, rather than just change their size. For clear identification of superconducting phases, low temperatures are required. This is particularly true for those cases which have zeros of the order parameter on the Fermi surface (which includes the three examples we treated). For these, the density of excited quasiparticles is proportional to a power of T for low T, rather than showing the activated behavior typical of a gap which is everywhere nonzero.

A natural direction in which to extend our work is towards the calculation of spin fluctuation free energies. It is now generally accepted that spin fluctuations play a decisive role in determining the relative stability of the superfluid phases of ^{3}He.[15] Since the susceptibilities of heavy-fermion materials are strongly enhanced, we expect this mechanism also to be important for these systems. This contribution to the free energy is a functional only of $\chi(\mathbf{q},\omega)$ so we have in principle the means of determining it. However, uncertainty at the present time about the nature of the fluctuation spectrum in the normal state makes this program difficult. The authors of Ref. 15 considered paramagnon fluctuations which were large only near $\mathbf{q}=\mathbf{0}$. In evaluating χ in the superconducting state, they were then able to neglect the distinction between d_+ and d_- while performing the sums over $\mathbf{k}$. One can then make progress analytically and derive criteria for the stability of states by determining the parameters of a Landau expansion of the free energy. In the heavy-fermion case, on the other hand, there is experimental evidence[12] which indicates that the normal state fluctuations are not well localized near $\mathbf{q}=\mathbf{0}$. Theoretically, there are reasons to expect that antiferromagnetic fluctuations may be important in heavy-fermion systems. This stems from the fact that most pictures of these systems postulate a narrow band of highly correlated f electrons which is almost half filled.[26] It is therefore very close to the half-filled, large-U Hubbard model, which is known to be antiferromagnetic.[27] In addition the Curie-Weiss susceptibility at high temperatures is that characteristic of an antiferromagnet, i.e., it has a negative intercept on the T axis of a graph of χ^{-1} versus T.

For these different possibilities for normal state fluctuations, in particular when it is not possible to neglect the difference between d_+ and d_-, the numerical labor involved in calculating spin fluctuation energies will be onerous, and it is left for the future.

We conclude that neutron scattering will be a uniquely efficacious tool for the identification of unconventional superconducting phases. The study of the anisotropy of scattering intensities as a function of scattering angle gives detailed information about the magnitude of the gap as a function of position of the Fermi surface. If polarization analysis is added to the experiment, even the vector structure of the order parameter as a function of position can in principle be determined. The magnetic properties of heavy-fermion systems may also be important for the question of the relative stability of the various superconducting phases. In a strong magnetic field, the static susceptibility could play a role. In particular, it would be interesting to investigate the phase diagram of $U_{1-x}Th_xBe_{13}$ as a function of field in greater detail. A start on this has been made.[28] But more particularly, one would like to see this done also as a function of the direction of the field with respect to the crystal axes in single-crystal samples. This would help to understand which phases are actually realized in this alloy system. In the high-T_c systems, the large gap renders the proposed experiments much easier to realize. The structure of the order parameter in both spin and momentum space can be probed in the most detail by neutron scattering. Recent results[29] on single-phase nonsuperconducting La_2CuO_4 raise the hope that the clarification of the nature of high-T_c superconductivity by this method may lie in the near future.

[1]F. Steglich, J. Aarts, C. D. Bredl, W. Lieke, D. Meschede, W. Franz, and J. Schäfer, Phys. Rev. Lett. **43**, 1892 (1979).

[2]H. R. Ott, H. Rudigier, Z. Fisk, and J. L. Smith, Phys. Rev. Lett. **50**, 1595 (1983).

[3]G. R. Stewart, Z. Fisk, J. O. Willis, and J. L. Smith, Phys. Rev. Lett. **52**, 929 (1984).

[4]F. Steglich, in *Proceedings of the Eighth Taniguchi Symposium on Heavy Fermions and Valence Fluctuations, Shima, Japan, 1985*, edited by T. Kasuya (Springer, Berlin, 1986).

[5]H. R. Ott, H. Rudigier, T. M. Rice, K. Ueda, Z. Fisk, and J. L. Smith, Phys. Rev. Lett. **52**, 1915 (1984).

[6]D. J. Bishop, C. M. Varma, B. Batlogg, E. Bucher, Z. Fisk, and J. L. Smith, Phys. Rev. Lett. **53**, 1009 (1984) used a polar state to explain their ultrasonic attenuation data. This interpretation is further discussed in C. J. Pethick and D. Pines, Phys. Rev. Lett. **57**, 118 (1986); S. Schmitt-Rink, K. Miyake, and C. M. Varma, *ibid.* **57**, 2575 (1986); S. N. Coppersmith and R. A. Klemm, *ibid.* **56**, 1870 (1986); P. Hirschfeld, D. Vollhardt, and P. Wölfle, Solid State Commun. **59**, 111 (1986); K. Scharnberg, D. Walker, H. Monien, L. Tewordt, and R. A. Klemm, *ibid.* **60**, 535 (1986); L. Coffey, Phys. Rev. B **35**, 8440 (1987).

[7]G. J. Bednorz and K. A. Müller, Z. Phys. B **64**, 189 (1986).

[8]M. K. Wu, J. R. Ashburn, C. J. Torng, P. H. Hor, R. L. Meng, L. Gao, Z. J. Huang, Y. Q. Wang, and C. W. Chu, Phys. Rev. Lett. **58**, 908 (1987).

[9]A. Ruckenstein, P. Hirschfeld, and J. Appel, Phys. Rev. B **36**, 857 (1987).

[10]G. Kotliar, Phys. Rev. B **37**, 3664 (1988); H. J. Schulz, Europhys. Lett. **4**, 609 (1987); P. A. Lee and N. Read, Phys. Rev.

Lett. **58**, 2691 (1987).
[11]C. Gros, R. Joynt, and T. M. Rice, Z. Phys. B **68**, 425 (1987); C. Gros (unpublished).
[12]A. I. Goldman, G. Shirane, G. Aeppli, G. Bucher, and J. Hufnagl, J. Magn. Magn. Mater. **63–64**, 380 (1987).
[13]L. Taillefer, R. Newbury, G. G. Lonzarich, Z. Fisk, and J. L. Smith, J. Magn. Magn. Mater. **63-64**, 372 (1987).
[14]J. D. Axe and G. Shirane, Phys. Rev. Lett. **30**, 214 (1973); Phys. Rev. B **8**, 1965 (1973).
[15]W. F. Brinkman, J. W. Serene, and G. P. W. Anderson, Phys. Rev. A **10**, 2386 (1974).
[16]S. Takagi, Ph.D. thesis, University of Tokyo, 1973, quoted in A. J. Leggett, Rev. Mod. Phys. **47**, 331 (1975).
[17]P. W. Anderson, Phys. Rev. B **30**, 4000 (1984).
[18]G. E. Volovik and L. P. Gor'kov, Pis'ma Zh. Teor. Fiz. **39** 550 (1984) [JETP Lett. **39**, 674 (1984)]; Zh. Eksp. Teor. Fiz. **88**, 1412 (1985) [Sov. Phys. JETP **61**, 843 (1985)].
[19]K. Ueda and T. M. Rice, Phys. Rev. B **31**, 7114 (1985).
[20]E. I. Blount, Phys. Rev. B **32**, 2935 (1985).
[21]M. Cyrot, Solid State Commun. **60**, 253 (1986); D. J. Scalapino, E. J. Loh, Jr., and J. E. Hirsch, Phys. Rev. B **34**, 8190 (1986); K. Miyake, S. Schmitt-Rink, and C. M. Varma, *ibid.* **34**, 5736 (1986); also see F. C. Zhang and T. K. Lee, *ibid.* **35**, 3651 (1987).
[22]Z. Zou and P. W. Anderson, Phys. Rev. Lett. **57**, 2073 (1986); **58**, 2731 (1987); also see F. C. Zhang and T. K. Lee, *ibid.* **58**, 2728 (1987); G. Aeppli and C. M. Varma, *ibid.* **58**, 2729 (1987); D. Cox, *ibid.* **58**, 2730 (1987).
[23]R. Heffner, *Proceedings of the Fifth International Conference on Valence Fluctuations, Bangalore, 1987* (Plenum, New York, in press).
[24]R. A. Ferrell, Phys. Rev. Lett. **3**, 262 (1959); P. W. Anderson, *ibid.* **3**, 325 (1959).
[25]K. Ueda and T. M. Rice, in *Proceedings of the Eighth Taniguchi Symposium on Heavy Fermions and Valence Fluctuations, Shima, Japan, 1985,* edited by T. Kasuya (Springer, Berlin, 1986).
[26]P. A. Lee, T. M. Rice, J. W. Serene, J. L. Sham, and J. W. Wilkins, Comments Cond. Mat. Phys. **XII**, 99 (1986); C. M. Varma, *ibid.* **XI**, 221 (1985), review the theories.
[27]C. Gros, R. Joynt, and T. M. Rice, Phys. Rev. B **36**, 381 (1987).
[28]H. R. Ott, Rudigier, G. Felder, Z. Fisk, and J. L. Smith, Phys. Rev. B **33**, 126 (1986).
[29]G. Shirane, Y. Endoh, R. J. Birgeneau, M. A. Kastner, Y. Hidaka, M. Oda M. Suzuki, and T. Murakami, Phys. Rev. Lett. **59**, 1613 (1987).